Multistage pressure-retarded osmosis configurations: A unifying framework and thermodynamic analysis

Multistage pressure-retarded osmosis configurations: a unifying framework and thermodynamic analysis

Hyung Won Chung[a], Jaichander Swaminathan[b], John H. Lienhard V[a,*]

[a] *Rohsenow Kendall Heat Transfer Laboratory, Department of Mechanical Engineering, Massachusetts Institute of Technology, Cambridge MA 02139-4307 USA*
[b] *Dr. Kiran C. Patel Center for Sustainable Development, Mechanical Engineering Discipline, IIT Gandhinagar, Gujarat, India 382355*

Abstract

Pressure-retarded osmosis has enjoyed increasing research interest over the last decade. Recent studies focusing on single-stage PRO designs have raised doubts regarding the long-term economic viability of the technology. While most of the analyses are based on single-stage operation, comprehensive analysis of multistage PRO which shows promise for better energetic performance is absent. Previous studies on multistage PRO differ in their design philosophies and performance metrics, leading to an incomplete assessment regarding the potential benefits of multistaging. In this paper, we develop a unifying framework to classify several existing multistage configurations. In addition, we analyze the multistage PRO system from a thermodynamic perspective. Among the two major multistage design strategies, namely interstage pressure control and independent feed inputs to each stage, we found the latter to be more effective towards increasing net power density. In comparison to a single-stage device, a 10-stage system achieves around 9% higher net power density while using the same membrane area.

Keywords: Pressure-retarded osmosis; salinity-gradient power; multistage; thermodynamic analysis; feed inputs

H.W. Chung, J. Swaminathan, and J.H. Lienhard V, "Multistage pressure-retarded osmosis configurations: a unifying framework and thermodynamic analysis," *Desalination*, online 28 November 2019, **476**:114230, 15 February 2020.

*Corresponding author: lienhard@mit.edu

Nomenclature

A	Permeability constant, L/m^2-hr-bar
A_m	Membrane area, m^2
B	Salt diffusion constant, L/m^2-hr
d_ch	Channel depth, m
f	Friction factor
h	Specific enthalpy of seawater, J/kg
J_w	Water flux, kg/m^2-hr
J_s	Salt flux, kg/m^2-hr
L	Membrane length, m
$\dot{m}_\mathrm{d}$	Mass flow rate of draw stream, kg/s
$\dot{m}_\mathrm{f}$	Mass flow rate of feed stream, kg/s
P_d	Pressure of draw stream, bar
$P_\mathrm{den,net}$	Net power density, W/m^2
P_f	Pressure of feed stream, bar
P^*	Dimensionless pressure
$\dot{Q}_0$	Heat transfer to the environment, W
s	Specific entropy of seawater, J/kg-K
S	Structural parameter, μm
$\dot{S}_\mathrm{gen}$	Entropy generation rate, W/K
w_d	Draw salinity, g/kg
w_f	Feed salinity, g/kg
$\dot{W}_\mathrm{module}$	Gross power output from the PRO module, W
$\dot{W}_\mathrm{net}$	Net power, W
$\dot{W}_\mathrm{p,f}$	Pump power consumption of feed stream, W
$\dot{W}_\mathrm{p,d}$	Pump power consumption of draw stream, W
$\dot{W}_\mathrm{t}$	Turbine power output, W
π	Osmotic pressure, bar
ρ_d	Density of draw stream, kg/m^3
ξ	Specific flow exergy of seawater, J/kg
$\Delta\dot{\Xi}_\mathrm{streams}$	Net exergy input to the system, W

1. Introduction

As recent studies [1, 2] have found potential links between climate change and natural disasters, the need for renewable energy technologies is rapidly growing. Mature renewable technologies such as wind or solar have an inherent disadvantage since they are intermittent and cannot be used as a reliable source of base load power, without additional energy storage. Salinity-gradient power technology, in contrast, is non-intermittent renewable technology. Two major technologies for capturing salinity-gradient power are pressure-retarded osmosis (PRO) and reverse electrodialysis (RED). Yip et al. [3] found that PRO has both higher efficiency and power density.

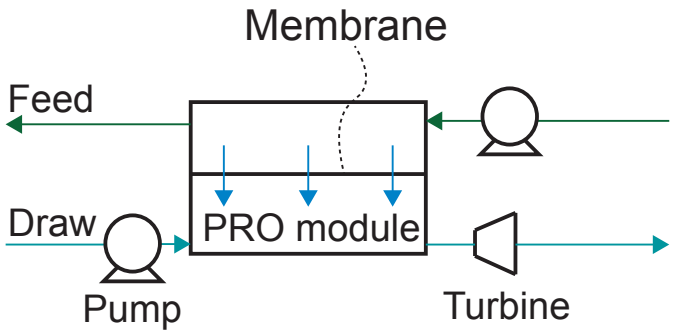

Figure 1: Basic components of PRO process

The minimal components required for the PRO process is shown in Fig. 1. Draw stream is a more concentrated than the feed stream. The PRO module is effectively a counterflow mass exchanger where the two channels are separated by a membrane that allows water to pass through while rejecting significant portion of the solutes. The draw stream is pressurized to a pressure less than its osmotic pressure before entering the module. Because of the salinity difference, water is drawn to the draw side. The draw stream is run through a turbine after exiting the PRO module. Because of the increased flow rate, the energy extracted from the turbine can be larger than what was required to pressurize the draw stream in the pump, hence generating net positive energy.

PRO has received significant interest from researchers around the world as evidenced by the rapidly increasing number of publications on the topic [4]. Notwithstanding this research interest, PRO has not yet been successfully commercialized. The only major attempt at commercialization was by Statkraft [5, 6], which closed operations in 2014. In order to develop PRO as a commercially viable technology, researchers should strive toward improving a performance metric that directly relates to the economics of PRO as a power production technology. While power density is widely used as a performance metric [7–10], Chung et al. [11] recently found that net power density is a more useful performance metric because it captures both the economic and energetic aspects of a PRO system. In this manuscript, we evaluate multistage operation as a means to improve net power density of PRO.

The vast majority of the studies and tests have focused on single-stage PRO (including large pilot plants such as Japan's Megaton Project). Multistage operation results in improved energetic performance in related processes such as reverse osmosis [12] and has the potential to outperform conventional single-stage PRO. Research into multistaging of PRO for improved performance is still in its infancy, with no clear multistage configurations identified for maximizing PRO performance. This is because researchers [13–16] have used different performance metrics and analyzed contrasting multistage configurations without sufficient theoretical justification or a common design philosophy. This makes it difficult to compare different multistage designs available in the literature in a coherent manner. The goals of this paper are therefore to theoretically analyze multistage systems and to develop an optimal design strategy. We establish a unified design taxonomy for multistage PRO system and apply thermodynamic analysis to three different multistage configurations. We then compare the three configurations to a baseline single-stage model to determine the optimal design.

2. Model description

We follow the modeling approach described in detail in Chung et al. [17]. The major building blocks of the model are summarized here. Since we want to capture property variations in the flow direction (i.e., the x direction), we define a differential control volume as shown in Fig. 2. The water mass balance for the control volume in the draw channel yields

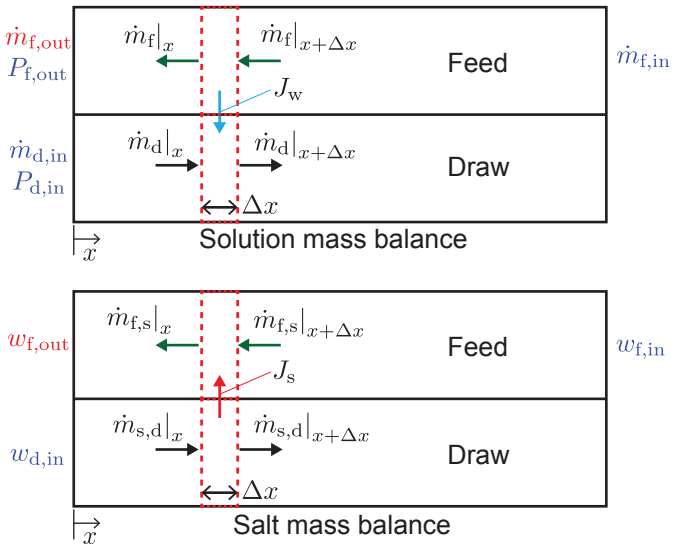

Figure 2: Differential control volume.

$$\dot{m}_d|_{x+\Delta x} - \dot{m}_d|_x = J_w d_{ch} \Delta x. \tag{1}$$

where J_w is water flux and d_{ch} is the channel depth (into the page). By Taylor series expansion, we have

$$\dot{m}_d|_{x+\Delta x} = \dot{m}_d|_x + \frac{d\dot{m}_d}{dx}\Delta x + O\left(\Delta x^2\right). \tag{2}$$

Then, we can substitute $\dot{m}_d|_{x+\Delta x}$ into the mass balance equation and let Δx approach zero to obtain

$$\frac{d\dot{m}_d}{dx} = J_w d_{ch}. \tag{3}$$

Applying the same procedure to the feed channel, we et

$$\frac{d\dot{m}_f}{dx} = J_w d_{ch}. \tag{4}$$

We can also apply the mass balance on the salt stream, which results in

$$\frac{d\dot{m}_{d,s}}{dx} = -J_s d_{ch} \tag{5}$$

and

$$\frac{d\dot{m}_{f,s}}{dx} = -J_s d_{ch}. \tag{6}$$

where J_s is the salt flux. The viscous pressure drop in the draw and feed channels can be expressed using the friction factor, f, as follows.

$$\frac{dP_d}{dx} = -f\frac{1}{2}\rho_d v_d^2 \frac{1}{d_h} \tag{7}$$

$$\frac{dP_{\mathrm{f}}}{dx} = f\frac{1}{2}\rho_{\mathrm{f}} v_{\mathrm{f}}^2 \frac{1}{d_{\mathrm{h}}}. \tag{8}$$

The mass transfer processes can be implicitly described by Eqs. (9) to (12) (see [17] details).

$$J_{\mathrm{w}} = A\rho\left[(\pi_{\mathrm{d,m}} - P_{\mathrm{d,m}}) - (\pi_{\mathrm{f,m}} - P_{\mathrm{f,m}})\right] \tag{9}$$

$$J_{\mathrm{s}} = B\rho\left(w_{\mathrm{d,m}} - w_{\mathrm{f,m}}\right) \tag{10}$$

$$w_{\mathrm{d,m}} = w_{\mathrm{d,b}} \exp\left(-\frac{J_{\mathrm{w}}}{\rho k}\right) - \frac{B\left(w_{\mathrm{d,m}} - w_{\mathrm{f,m}}\right)}{J_{\mathrm{w}}}\left[1 - \exp\left(-\frac{J_{\mathrm{w}}}{\rho k}\right)\right] \tag{11}$$

$$w_{\mathrm{f,m}} = w_{\mathrm{f,b}} \exp\left(\frac{J_{\mathrm{w}} S}{\rho D}\right) - \frac{B\left(w_{\mathrm{d,m}} - w_{\mathrm{f,m}}\right)}{J_{\mathrm{w}}}\left[\exp\left(\frac{J_{\mathrm{w}} S}{\rho D}\right) - 1\right] \tag{12}$$

where A is membrane permeability constant, B is the salt diffusion coefficient, S is the structural parameter and D is the average diffusion coefficient of NaCl. Here we use an average value of $D = 1.52 \times 10^{-9}$ m^2/s [18]. A membrane from Hydration Technology Innovation was used as the basis for membrane properties. Straub et al. [8] investigated this membrane and reported that $A = 2.49$ L/m^2-hr-bar, $B = 0.39$ L/m^2-hr and $S = 564$ µm.

Equations (3) to (8) are coupled-linear ordinary differential equations that need to be solved simultaneously along with Eqs. (9) to (12). Solving these equations completely specifies a single stage PRO system. In other words, mass flow rate, salinity and pressure at any position x is specified. From this we can calculate energy consumption in the pump and energy output of the turbine. We can use appropriate continuity condition (e.g., flow rate out of stage 1 is equal to the flow rate into stage 2 if no processing occurs between stages) to build a multistage models. To solve these equations, scikits .bvp_solver [19] was used.

3. Multistage PRO

In this section, we investigate multistage PRO in more detail. First, existing studies on multistage systems are reviewed in Section 3.1, focusing on the multistage flow configurations considered therein and the performance metrics used to evaluate competing designs. Then, in Section 3.2, we define two strategies for desinging multistage systems. Based on these two strategies, we define a unified multistage design taxonomy and classify existing systems using this general framework in Section 3.3.

3.1. Multistage designs in the literature

He et al. [14] introduced four dual-stage designs as shown in Fig. 3. The design (a) is equivalent to a single stage system with length equal to the sum of the two stages. The design (b) is equivalent to a single stage design with the width the same as the sum of two stages. Hence, we will not consider these two systems as multistage. For the design (c), the same feed stream is used in both stages. We analyze this kind of system in Section 3.2.2. The design (d) uses the same draw stream in both stages. The ratio of module power output (as opposed to net power) to the permeate flow rate $\frac{\dot{W}_{\mathrm{module}}}{Q_{\mathrm{p}}}$, was used as the performance metric. The most promising salinity pairing for PRO is an ultrasaline brine as draw with an impaired water stream such as domestic wastewater as feed [11]. Using a separate draw input to each stage would require a higher quantity of ultrasaline brine input, which would have to be rejected from the system at lower dilution and which may not meet discharge regulations.

Altaee and Hilal [20] studied the dual-stage PRO system shown in Fig. 4. An important feature of this design is the booster pressure pump between the stages. This pump pressurizes the draw stream leaving the first stage before entering the second stage. They used module power density, P_{den}, as a performance metric.

Bharadwaj et al. [16] analyzed a more general multistage system as shown in Fig. 5. In particular, turbines between successive stages depressurize the draw stream, in contrast to the booster pump in Fig. 4. They used $\frac{\dot{W}_{\mathrm{net}}}{Q}$, a ratio of net power to a flow rate (either feed or draw stream), as a performance metric.

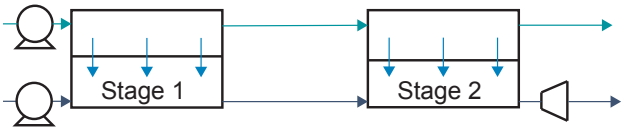

(a) The second stage directly takes input from the first stage. Design (a) is effectively a single stage.

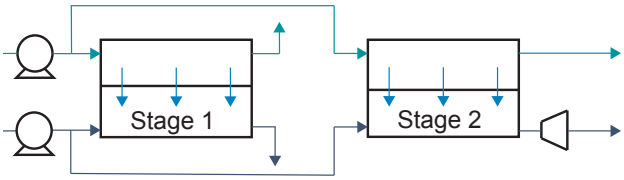

(b) Same feed and draw streams are introduced in each stage.

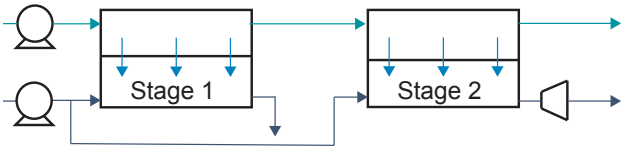

(c) The same draw stream is used in both stages.

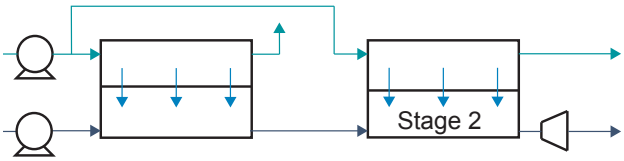

(d) The same feed stream is used in both stages.

Figure 3: Dual-stage designs in [14].

However, they did not consider the viscous pressure drop inside the module. In Section 4.1, we analyze whether interstage pressurization or depressurization should be used.

The last multistage study we analyze is by Li [13] shown in Fig. 6. Similar to [16], this system has interstage depressurization using turbines. Li used normalized specific energy production defined as NSEP $\triangleq \frac{\dot{W}_{\text{net}}}{\dot{Q}_{\text{d,in}}\pi_{\text{d,in}}}$ as a performance metric.

In all of these multistage studies, the authors achieved better performance than single stage systems. However, the performance metric used by each author is different, and it is unclear if the multistage system would necessarily outperform single-stage under a different metric. Moreover, none of those studies compared different multistaging approaches; they chose one design and presented it against the single-stage system. Hence, it is difficult to compare the disparate multistage configurations against one another. Different systems even have opposing design philosophies: interstage pressurization in [20] as opposed to interstage depressurization in [13, 16], as well as parallel [14, 16] vs. countercurrent [13, 20] flow of feed and draw streams.

In this paper, we aim to perform a head-to-head comparison of these multistage designs using net power density as a performance metric, as recommended in [11]. The theoretical underpinnings for variation in performance among the designs are explored via thermodynamic analysis in Section 4.

3.2. Multistage design strategies

In general, multistaging results in a more complicated system compared to a single-stage system, with additional degrees of freedom for system inputs and parameters. By optimizing these extra parameters with

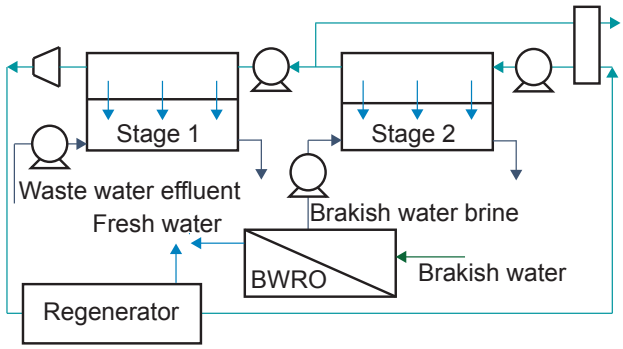

Figure 4: Dual-stage design in [20].

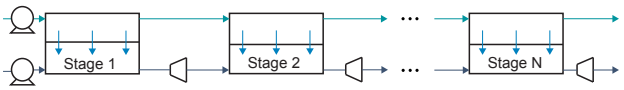

Figure 5: Multistage design in [16]. The flow configuration is parallel.

respect to a system performance, multistage systems outperform single stage systems. For the specific case of PRO, we can harness two extra degrees of freedom: interstage pressure control and input exergy control.

3.2.1. Interstage pressure control

A natural advantage of multistage designs is that the pressure of each stage can be independently chosen and set. The dual-stage designs in Figs. 4 to 6 all use one form of interstage pressure control.

An advantage of such pressure control is that it can help achieve a more uniform distribution of osmotic driving force, which can help reduce overall entropy generation in the system [21, 22]. Figure 7 qualitatively shows how multistaging achieves a more uniform osmotic driving force. The local osmotic driving force is defined as $\Delta\pi_{\mathrm{d}}(x) \triangleq \{\pi(w_{\mathrm{d}}(x)) - P_{\mathrm{d}}(x)\} - \{\pi(w_{\mathrm{f}}(x)) - P_{\mathrm{f}}(x)\}$ where $\pi(w)$ is the osmotic pressure of seawater at the salinity level of w (obtained here from a seawater properties library [23]). Note that the draw pressure drops with each subsequent stage ($P_{\mathrm{d},1} > P_{\mathrm{d},2} \ldots$) to realize a system with a more uniform driving force across the various stages.

3.2.2. Input exergy control

A multistage design allows for additional inflow and outflow options for the feed and draw streams, which has been utilized as a means to improve PRO performance. In thermodynamic terms, this corresponds to controlling the the net exergy input to the system. For example, in Design (c) in Fig. 3, the same feed stream is used in both stages which helps increase the salinity difference across the membrane in the second stage. The dual-stage design in Fig. 4 also corresponds to this category because a different feed stream is used in each stage (wastewater effluent in one stage and brackish water in the other) at different flow rates.

As shown in [24], controlling the feed exergy input to the system increases the thermodynamic maximum work that can be extracted from the salinity-gradient power systems such as PRO. This is how multistage systems with independent feed streams may attempt to improve performance. One caveat is that in [24], maximum thermodynamic work was analyzed without considering the system size necessary (a large area would be required to achieve thermodynamic maximum work output). In contrast, the performance metric

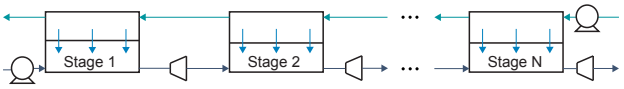

Figure 6: Multistage design in [13]. A counterflow configuration was used.

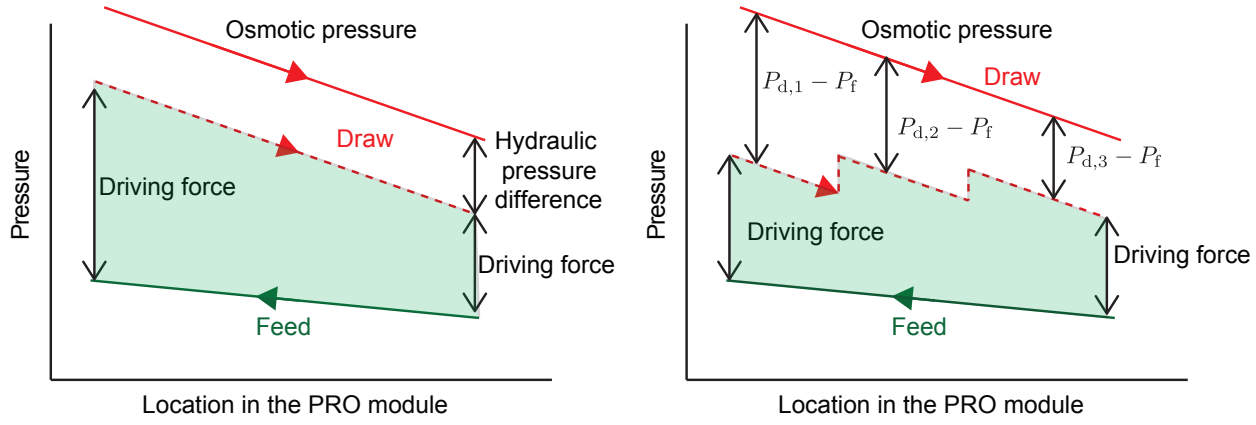

(a) Single-stage system

(b) Multistage system

Figure 7: Osmotic driving force distribution. Solid lines are osmotic pressure and dotted lines are hydraulic pressure. The hydraulic pressure for the feed stream is not shown for simplicity.

of interest in our case is net power density, which penalizes a large system area. Therefore, it is not obvious whether controlling the input feed streams can also improve net power density. We investigate this issue in Section 4.

3.3. Unified multistage design taxonomy

With interstage pressure and exergy input as control knobs, we can define a taxonomy to classify different multistage designs. Without loss of generality, we can illustrate this taxonomy using dual-stage system as shown in Fig. 8. On the right-hand-side of each system, there is a simple graph to indicate the design strategy of the dual-stage system. Note that in Fig. 8a there is an unspecified pressure control device; this can be either a turbine or a pump to achieve pressurization or depressurization. This general pressure control device allows us to directly compare systems such as those in [20] with [13, 16]. Pressure of the draw stream, after leaving stage 1, would be controlled such that the resulting net power density of the dual-stage system is increased.

The system shown in Fig. 8b corresponds to the feed exergy control and the one in Fig. 8c employs both interstage pressure and feed exergy controls.

With this general taxonomy, we can systematically classify existing multistage designs in the literature. In other words, the dual-stage systems in Fig. 8 represent a wide range of multistage systems. So in the following sections, we focus on the analysis of these general systems rather than analyzing each individual system proposed in the literature.

4. Thermodynamic analysis

In order to understand how interstage pressure and input exergy affects the multistage system, we first analyze the systems from a thermodynamic perspective. We use a single-stage system as our baseline model and make frequent comparison to it. In doing so, we use the same total area for both single-stage and dual-stage systems, i.e., the sum of the area of stage 1 and stage 2 is equal to the area of the single-stage system. Therefore, comparing these two systems in terms of net power is equivalent to comparing them in terms of net power density.

In this section, we focus on the salinity pairing of $w_f = 1$ g/kg and $w_d = 70$ g/kg. We assume a pump efficiency of 0.9. We assume that the interstage work transfer devices are isentropic such that the effect of interstage pressure control can be isolated from the irreversibility of the interstage turbine.

Figure 9 shows generic single-stage, dual-stage with interstage pressure control device and dual-stage with feed exergy control systems and their associated control volumes (CVs). The CVs are carefully chosen such that all streams enter and leave the control volume at the ambient temperature and pressure but at

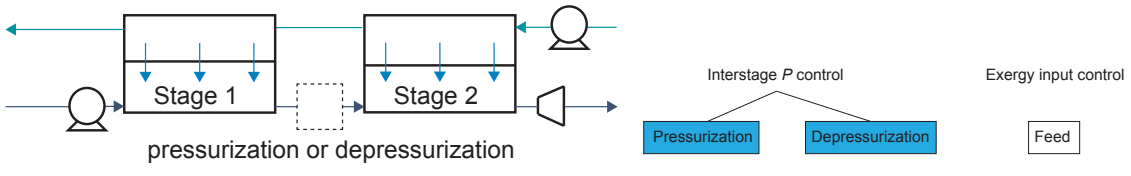

(a) Dual-stage with interstage pressure control.

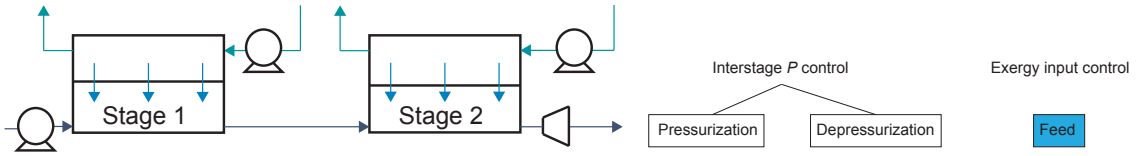

(b) Dual-stage with feed exergy control.

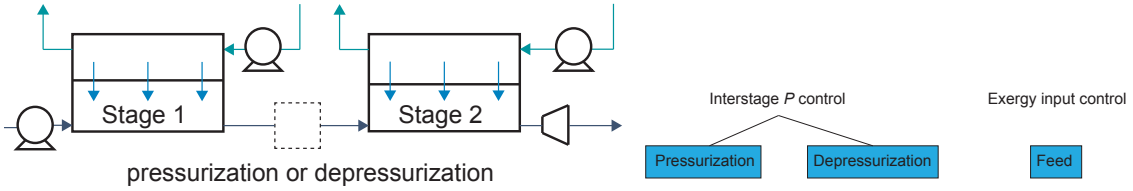

(c) Dual-stage with both interstage and feed exergy controls.

Figure 8: Dual-stage designs with taxonomy. Colored nodes in the taxonomy graph indicate which design strategy the corresponding dual-stage system employs. For the general pressure control device, we colored both pressurization and depressurization to imply that it is be either of the two (but not both).

different salinities (restricted dead state). The environment is the only thermal reservoir with which the streams interact and the CVs are defined such that the local temperature for any heat transfer interactions is that of the ambient.

Applying the First and Second Law of Thermodynamics on the CV in Fig. 9a, we get

$$\dot{m}_{\mathrm{f,in}} h_{\mathrm{f,in}} - \dot{m}_{\mathrm{f,out}} h_{\mathrm{f,out}} + \dot{m}_{\mathrm{d,in}} h_{\mathrm{d,in}} - \dot{m}_{\mathrm{d,out}} h_{\mathrm{d,out}} - \dot{W}_{\mathrm{net}} - \dot{Q}_0 = 0 \tag{13}$$

where $\dot{W}_{\mathrm{net}} \triangleq \dot{W}_{\mathrm{t}} - \dot{W}_{\mathrm{p,d}} - \dot{W}_{\mathrm{p,f}}$ and

$$\dot{m}_{\mathrm{f,in}} s_{\mathrm{f,in}} - \dot{m}_{\mathrm{f,out}} s_{\mathrm{f,out}} + \dot{m}_{\mathrm{d,in}} s_{\mathrm{d,in}} - \dot{m}_{\mathrm{d,out}} s_{\mathrm{d,out}} + \dot{S}_{\mathrm{gen}} - \frac{\dot{Q}_0}{T_0} = 0. \tag{14}$$

We can combine Eqs. (13) and (14) to get

$$\dot{W}_{\mathrm{net}} = \dot{m}_{\mathrm{f,in}} \underbrace{\xi_{\mathrm{f,in}}}_{h_{\mathrm{f,in}} - T_0 s_{\mathrm{f,in}}} - \dot{m}_{\mathrm{f,out}} \xi_{\mathrm{f,out}} + \dot{m}_{\mathrm{d,in}} \xi_{\mathrm{d,in}} - \dot{m}_{\mathrm{d,out}} \xi_{\mathrm{d,out}} - T_0 \dot{S}_{\mathrm{gen}} \tag{15}$$

$$= \Delta \dot{\Xi}_{\mathrm{streams}} - T_0 \dot{S}_{\mathrm{gen}} \tag{16}$$

where we define specific exergy of the streams as $\xi \triangleq h - T_0 s$ and refer to the net exergy rate input to the system as $\Delta \dot{\Xi}_{\mathrm{streams}}$. In fact, Eq. (16) also describes the Fig. 9b and Fig. 9c, if the definition of net power term is adjusted accordingly. For Fig. 9b, we define

$$\dot{W}_{\mathrm{net}} \triangleq \dot{W}_{\mathrm{t}} + \dot{W}_1 - \dot{W}_{\mathrm{p,d}} - \dot{W}_{\mathrm{p,f}} \tag{17}$$

where $\dot{W}_1$ is the work transfer term defined as positive when transferring from the system to the environment. In other words, $\dot{W}_1 > 0$ when the pressure control device is a turbine and $\dot{W}_1 < 0$ when it is a pump. The definition of $\dot{\Xi}_{\mathrm{streams}}$ stays the same.

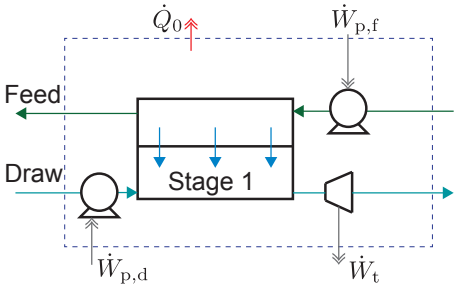

(a) Single-stage system and its CV.

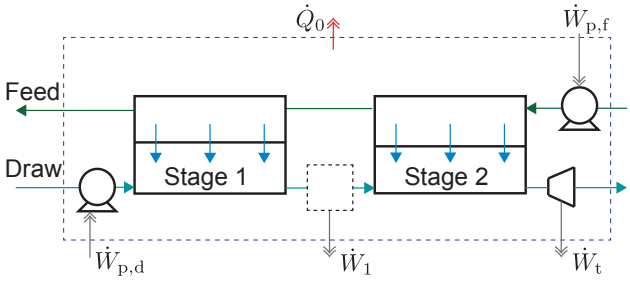

(b) Dual-stage system with pressure control device and its CV.

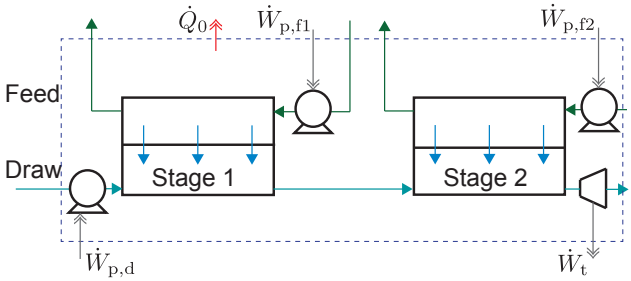

(c) Dual-stage system with pressure control device and its CV.

Figure 9: Control volume definitions for single-stage and dual-stage systems.

For Fig. 9c, we define

$$\dot{W}_{\mathrm{net}} \triangleq \dot{W}_{\mathrm{t}} - \dot{W}_{\mathrm{p,d}} - \dot{W}_{\mathrm{p,f1}} - \dot{W}_{\mathrm{p,f2}} \tag{18}$$

and

$$\dot{\Xi}_{\mathrm{streams}} \triangleq \dot{m}_{\mathrm{f,in1}}\xi_{\mathrm{f,in1}} - \dot{m}_{\mathrm{f,out1}}\xi_{\mathrm{f,out1}} + \dot{m}_{\mathrm{f,in2}}\xi_{\mathrm{f,in2}} - \dot{m}_{\mathrm{f,out2}}\xi_{\mathrm{f,out2}} + \dot{m}_{\mathrm{d,in}}\xi_{\mathrm{d,in}} - \dot{m}_{\mathrm{d,out}}\xi_{\mathrm{d,out}}. \tag{19}$$

We can combine these modifications to show that the system shown in Fig. 8c also achieves Eq. (16), but we skip the step.

Equation (16) suggests two different ways to increase $\dot{W}_{\mathrm{net}}$. First, we can increase $\Delta\dot{\Xi}_{\mathrm{streams}}$ or we can reduce the entropy generation. Also, we can harness both these effects with higher $\Delta\dot{\Xi}_{\mathrm{streams}}$ and lower entropy generation if they do complement each other. But for better understanding of multistaging process, we should study each term separately. We will show that interstage pressure control focuses on the latter term, whereas input exergy control as a design strategy focuses on increasing the former.

4.1. Interstage pressure control

We previously showed that interstage pressure control can be used to make the osmotic driving force more uniform. At the same average driving force, this would result in reduced entropy generation [21]. Therefore, we first compare the single-stage system (Fig. 9a) and dual-stage with interstage pressure control

(Fig. 9b) while holding $\Delta\dot{\Xi}_{\text{streams}}$ of both systems constant at the same value (for a fair comparison). The rational behind using the same value of $\Delta\dot{\Xi}_{\text{streams}}$ is task-oriented. In this case, the task is to extract energy while operating with the same pair of draw and feed stream undergoing the same salinity change. We want to determine whether single-stage or dual stage system extracts more energy. In a practical scenario, a constraint on $\Delta\dot{\Xi}_{\text{streams}}$ is possible if an environmental regulation requires the plant to discharge the draw stream at specific salinity.

In this scenario, minimizing the entropy generation rate is equivalent to maximizing net power. Doing so isolates the effect of interstage pressure control on the resulting net power. In practice, matching $\Delta\dot{\Xi}_{\text{streams}}$ between single stage and dual-stage means that flow rates at the draw inlet, draw outlet and feed inlet are matched [1].

After matching these system parameters, the single stage system is fully specified. In contrast, the dual-stage system has one degree of freedom: stage 1 inlet pressure, denoted as P_1 [2]. We use dimensionless version [25] defined as

$$P_1^* \triangleq \frac{P_{\text{d,in}} - P_{\text{f,in}}}{\pi_{\text{d,in}} - \pi_{\text{f,in}}} \tag{20}$$

in terms of stage 1 inlet quantities. Figure 10 shows the effect of varying P_1^* on net power density, entropy generation rate and the interstage work transfer. Note that $\dot{W}_1 > 0$ implies that the work transfer device acts as a turbine and $\dot{W}_1 > 0$ implies that it is a pump. When P_1^* is high (above about 0.52), we need to depressurize before stage 2 in order to match $\Delta\dot{\Xi}_{\text{streams}}$ of the single stage system. On the other hand, if P_1^* is low, we need to supplement (or pressurize) before stagle 2 for the same reason.

As shown in Fig. 10c, the interstage work transfer monotonically increases with P_1^*; if the draw stream enters the system at higher pressure, it can be depressurized more. Solid green lines represent the turbine case and the dotted blue lines represent the use of a pump. Because the work transfer device is different on either side (each with a different efficiency), we have a kink at $\dot{W}_1 = 0$ in Figs. 10b and 10c. Moreover, this point with $\dot{W}_1 = 0$ implies that the dual-stage system is equivalent to the single stage system because no pressure control is applied between stages. These points are marked as a star in Fig. 10.

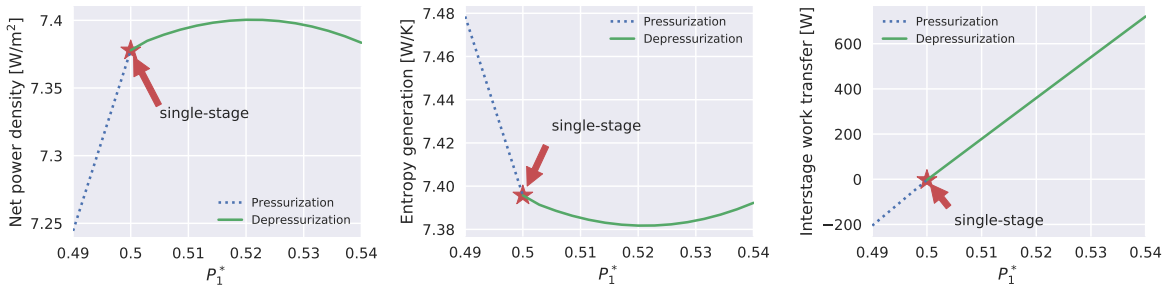

(a) $P_{\text{den,net}}$ (b) $\dot{S}_{\text{gen}}$ (c) $\dot{W}_1$

Figure 10: Dual-stage system with feed input exergy control (shown in Fig. 8a.)

Figure 10a shows that depressurization should be used instead of pressurization. This result confirms the qualitative analysis in Fig. 7 where $P_3 < P_2 < P_1$, implying that depressurization should be applied between stages in order to achieve a more uniform osmotic driving force. But the gain in net power density is not significant, and depressurizing beyond certain point (corresponding to $P_1^* \approx 0.52$) leads to a decrease in net power density. Figure 10b implies that as we move from pressurization to depressurization (with $P_1^* < 0.52$), the entropy generation decreases. This trend is expected because the system achieves a more uniform driving force.

This analysis suggests that the dual-stage system shown in Fig. 4 could have been improved if a turbine

[1] For this analysis, we assume that the salt diffusion coefficient of the membranes (B) is zero, which significantly simplifies the analysis.

[2] For each chosen value of P_1, there exists a unique value of P_2 that results in the same $\Delta\dot{\Xi}_{\text{streams}}$ between single and dual-stage systems, and we use such P_2.

	Single-stage	dual-stage in Fig. 8b	Dual-stage in Fig. 8c
$P_{\text{den,net}}$, W/m^2	6.68	6.96	6.96
$\dot{S}_{\text{gen}}$, W/K	9.760	10.063	10.061
$\Delta\dot{\Xi}_{\text{streams}}$, W	4145	4288	4288

Table 1: Dual-stage systems with input exergy control and interstage pressure control.

was used instead of a booster pump between the two stages.

4.2. Input exergy control

In this section, we compare a single-stage (Fig. 9a) and dual-stage PRO with independent feed input (Fig. 9c). Because an independent feed stream is introduced, it is not possible to match $\Delta\dot{\Xi}_{\text{streams}}$ between single and dual-stage systems as in Section 4.1[3]. In order to make a fair comparison, we fix the total area to be the same between the systems under comparison. Then, the remaining variables (draw and feed inlet velocities and inlet pressures) were optimized to maximize the resulting net power density (see [17] for more details on the optimization technique).

Table 1 shows the results. Dual-stage systems with independent feed streams in each stage result in higher entropy generation rate than for the single stage system. However, because $\Delta\dot{\Xi}_{\text{streams}}$ more than compensates for the increased entropy generation, the resulting net power density is higher for dual-stage systems. This suggests that unless a PRO system is operating under the constraint of a specific $\Delta\dot{\Xi}_{\text{streams}}$ value, minimizing entropy generation does not result in optimal operation. In a practical scenario, a constraint on $\Delta\dot{\Xi}_{\text{streams}}$ is possible if an environmental regulation requires the plant to discharge the draw stream at specific salinity.

Another important observation we can make from Table 1 is that interstage pressure control does not help much. Having a turbine between stages reduces the entropy generation by a small amount but the overall performance gain is zero up to two significant digits after the decimal point. From this analysis, we conclude that the dual-stage design is better than the single-stage system and that dual-stage design without interstage pressure control is the recommended configuration as it captures most of the benefit of multistaging.

5. Optimal multistage design

From the analysis in Section 4, we suggest the optimal multistage configuration shown in Fig. 11. This

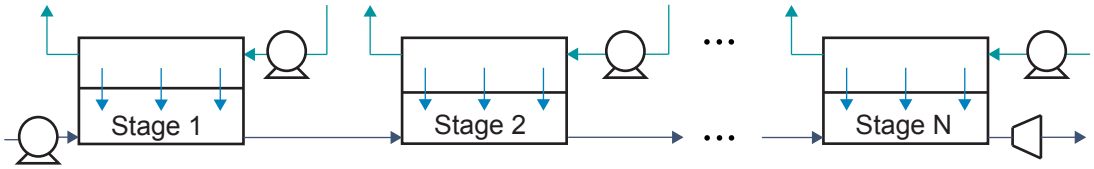

Figure 11: Optimal multistage design.

system uses an independent feed stream in each stage. Although we focused on two-stage systems in Section 4, we can extend the analysis to N stages with $N > 2$. Figure 12 shows how net power density changes as the number of stages increases. For this plot, we fixed the total system size to be the same for all points. For example, if single-stage system has length of 5 m, then 10-stage system has length of 0.5 m in each stage. All free parameters (e.g., feed inlet velocities) were chosen such that the net power density is maximized.

As shown in Fig. 12, there exist strong diminishing returns. Four stages seem to be enough to capture most of the benefits of multistaging while keeping the device operation relatively simple. A 10-stage system

[3]Another difference between this section and Section 4.1 is that, we use $B = 0.39$ L/m^2-hr instead of 0. This results in slightly lower net power density.

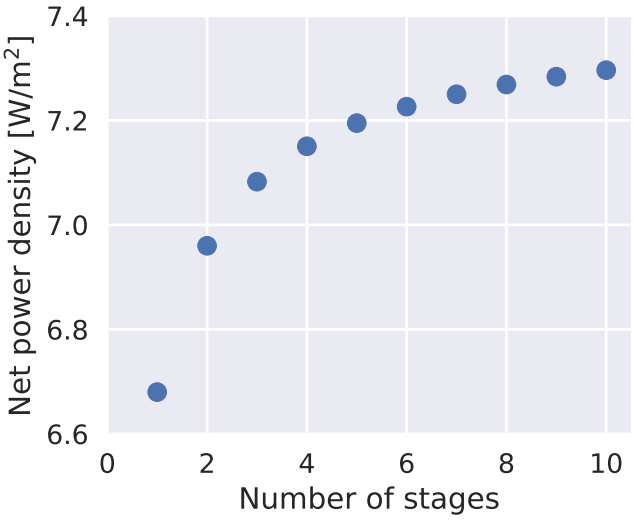

Figure 12: Effect of number of stages on net power density.

achieves about 9.1% higher net power density compared to the single-stage while 4-stage system achieves 7.0% improvement. Ultimately, the system designer should determine the tradeoff between system complexity, net power density and capital costs.

6. Conclusion

A comprehensive analysis of various multistage PRO configurations has been presented, starting with a survey of the literature followed by a thermodynamic analysis of two-stage systems. The primary conclusions are as follow:

- Inconsistent multistage design philosophies and evaluation metrics exist in the literature, which have prevented the identification of an optimal PRO design.
- Two major design strategies with respect to multistaging of PRO were identified: one based on adjusting the input streams and one based on adjusting the draw pressure in each stage. This understanding leads to a comprehensive multistage design taxonomy which enables the succinct classification of a wide range of multistage designs
- When controlling the interstage draw solution pressure change, depressurization from one stage to a following stage is strictly better than pressurization.
- Controlling the exergy input is a more effective way to increase net power density of PRO.
- An optimal multistage design (from a practical standpoint) uses an independent feed stream in each stage without an interstage pressure control.

7. Acknowledgements

The authors would like to thank Kuwait Foundation for the Advancement Sciences (KFAS) for their financial support through Project No. P31475EC01.

References

[1] S. Ornes, Core concept: How does climate change influence extreme weather? impact attribution research seeks answers, Proceedings of the National Academy of Sciences 115 (33) (2018) 8232–8235. arXiv:https://www.pnas.org/content/115/33/8232.full.pdf, doi:10.1073/pnas.1811393115.
URL https://www.pnas.org/content/115/33/8232

[2] M. D. Risser, M. F. Wehner, Attributable human-induced changes in the likelihood and magnitude of the observed extreme precipitation during hurricane harvey, Geophysical Research Letters 44 (24) (2017) 12,457–12,464. arXiv:https://agupubs.onlinelibrary.wiley.com/doi/pdf/10.1002/2017GL075888, doi:10.1002/2017GL075888.
URL https://agupubs.onlinelibrary.wiley.com/doi/abs/10.1002/2017GL075888

[3] N. Y. Yip, M. Elimelech, Comparison of energy efficiency and power density in pressure retarded osmosis and reverse electrodialysis, Environmental Science & Technology 48 (18) (2014) 11002–11012. doi:10.1021/es5029316.
URL https://doi.org/10.1021/es5029316

[4] J. Kim, K. Jeong, M. J. Park, H. K. Shon, J. H. Kim, Recent advances in osmotic energy generation via pressure-retarded osmosis (PRO): A review, Energies 8 (10) (2015) 11821–11845. doi:10.3390/en81011821.
URL http://www.mdpi.com/1996-1073/8/10/11821

[5] S. E. Skilhagen, J. E. Dugstad, R. J. Aaberg, Osmotic power — power production based on the osmotic pressure difference between waters with varying salt gradients, Desalination 220 (1–3) (2008) 476 – 482, european Desalination Society and Center for Research and Technology Hellas (CERTH), Sani Resort 22 –25 April 2007, Halkidiki, GreeceEuropean Desalination Society and Center for Research and Technology Hellas (CERTH), Sani Resort. doi:http://dx.doi.org/10.1016/j.desal.2007.02.045.
URL http://www.sciencedirect.com/science/article/pii/S0011916407006467

[6] K. Gerstandt, K.-V. Peinemann, S. E. Skilhagen, T. Thorsen, T. Holt, Membrane processes in energy supply for an osmotic power plant, Desalination 224 (1) (2008) 64 – 70. doi:10.1016/j.desal.2007.02.080.
URL http://www.sciencedirect.com/science/article/pii/S0011916408000325

[7] G. Z. Ramon, B. J. Feinberg, E. M. V. Hoek, Membrane-based production of salinity-gradient power, Energy & Environmental Science 4 (2011) 4423–4434. doi:10.1039/C1EE01913A.
URL http://dx.doi.org/10.1039/C1EE01913A

[8] A. P. Straub, N. Y. Yip, M. Elimelech, Raising the bar: Increased hydraulic pressure allows unprecedented high power densities in pressure-retarded osmosis, Environmental Science & Technology Letters 1 (1) (2014) 55–59. arXiv:http://dx.doi.org/10.1021/ez400117d, doi:10.1021/ez400117d.
URL http://dx.doi.org/10.1021/ez400117d

[9] A. P. Straub, S. Lin, M. Elimelech, Module-scale analysis of pressure retarded osmosis: Performance limitations and implications for full-scale operation, Environmental Science & Technology 48 (20) (2014) 12435–12444.

[10] A. Achilli, J. L. Prante, N. T. Hancock, E. B. Maxwell, A. E. Childress, Experimental results from RO-PRO: A next generation system for low-energy desalination, Environmental Science & Technology 48 (11) (2014) 6437–6443. arXiv:http://dx.doi.org/10.1021/es405556s, doi:10.1021/es405556s.
URL http://dx.doi.org/10.1021/es405556s

[11] H. W. Chung, J. Swaminathan, L. D. Banchik, J. H. Lienhard, Economic framework for net power density and levelized cost of electricity in pressure-retarded osmosis, Desalination 448 (2018) 13–20. doi:10.1016/j.desal.2018.09.007.
URL http://www.sciencedirect.com/science/article/pii/S0011916418307537

[12] Q. J. Wei, R. K. McGovern, J. H. Lienhard, Saving energy with an optimized two-stage reverse osmosis system, Environmental Science: Water Research & Technology 3 (4) (2017) 659–670. doi:10.1039/C7EW00069C.

[13] M. Li, Systematic analysis and optimization of power generation in pressure retarded osmosis: Effect of multistage design, AIChE Journal 64 (1) (2018) 144–152. doi:10.1002/aic.15894.
URL http://dx.doi.org/10.1002/aic.15894

[14] W. He, Y. Wang, M. H. Shaheed, Enhanced energy generation and membrane performance by two-stage pressure retarded osmosis (PRO), Desalination 359 (2015) 186–199. doi:10.1016/j.desal.2014.12.014.
URL http://www.sciencedirect.com/science/article/pii/S0011916414006523

[15] A. Altaee, G. Zaragoza, A. Sharif, Pressure retarded osmosis for power generation and seawater desalination: Performance analysis, Desalination 344 (2014) 108 – 115. doi:10.1016/j.desal.2014.03.022.
URL http://www.sciencedirect.com/science/article/pii/S0011916414001581

[16] D. Bharadwaj, T. M. Fyles, H. Struchtrup, Multistage pressure-retarded osmosis, Journal of Non-Equilibrium Thermodynamics 41 (4) (2016) 327–347. doi:10.1515/jnet-2016-0017.
URL https://www.degruyter.com/abstract/j/jnet.2016.41.issue-4/jnet-2016-0017/jnet-2016-0017.xml

[17] H. W. Chung, L. D. Banchik, J. Swaminathan, J. H. Lienhard, On the present and future economic viability of stand-alone pressure-retarded osmosis, Desalination 408 (2017) 133 – 144. doi:10.1016/j.desal.2017.01.001.
URL http://www.sciencedirect.com/science/article/pii/S001191641631387X

[18] R. A. Robinson, R. H. Stokes, Electrolyte solutions, 2nd Edition, Dover Publications, 2002.

[19] scikits.bvp_solver, online; accessed Sep. 10, 2019. [link].
URL https://pythonhosted.org/scikits.bvp_solver/

[20] A. Altaee, N. Hilal, Dual stage PRO power generation from brackish water brine and wastewater effluent feeds, Desalination 389 (2016) 68–77. doi:10.1016/j.desal.2015.03.033.
URL http://www.sciencedirect.com/science/article/pii/S0011916415002003

[21] D. Tondeur, E. Kvaalen, Equipartition of entropy production. an optimality criterion for transfer and separation processes, Industrial & engineering chemistry research 26 (1) (1987) 50–56. doi:10.1021/ie00061a010.

[22] J. H. Lienhard, Energy savings in desalination technologies: Reducing entropy generation by transport processes, Journal of Heat Transfer 141 (7). doi:10.1115/1.4043571.

[23] K. G. Nayar, M. H. Sharqawy, L. D. Banchik, J. H. Lienhard, Thermophysical properties of seawater: A review and new correlations that include pressure dependence, Desalination 390 (2016) 1 – 24. doi:10.1016/j.desal.2016.02.024.
URL http://www.sciencedirect.com/science/article/pii/S0011916416300807

[24] H. W. Chung, K. G. Nayar, J. Swaminathan, K. M. Chehayeb, J. H. Lienhard, Thermodynamic analysis of brine management methods: Zero-discharge desalination and salinity-gradient power production, Desalination 404 (2017) 291 – 303. doi:10.1016/j.desal.2016.11.022.
URL http://www.sciencedirect.com/science/article/pii/S0011916416310396

[25] L. D. Banchik, M. H. Sharqawy, J. H. Lienhard, Limits of power production due to finite membrane area in pressure retarded osmosis, Journal of Membrane Science 468 (2014) 81 – 89. doi:http://dx.doi.org/10.1016/j.memsci.2014.05.021.
URL http://www.sciencedirect.com/science/article/pii/S037673881400386X